REPORT DOCUMENTATION PAGE

AFRL-SR-AR-TR-02-

0171

1. AGENCY USE ONLY *(Leave blank)*	2. REPORT DATE	3. REPO
	16 Apr 02	FINAL REPORT 01 Apr 00 to 30 Sep 01

4. TITLE AND SUBTITLE
EQUIPMENT FOR SYSTEM DEMONSTRATION OF PHASED ARRAY ANTENNA USING POLYMER-BASED OPTICAL TRUE TIME DELAY MODULE

5. FUNDING NUMBERS
F49620-00-1-0250

3484/US

61103D

6. AUTHOR(S)
Dr Ray T. Chen

7. PERFORMING ORGANIZATION NAME(S) AND ADDRESS(ES)
University of Texas at Austin
Microelectronics Research Certer
10100 Burnet Road, Bldg. 160
Austin, TX 78758

8. PERFORMING ORGANIZATION REPORT NUMBER

9. SPONSORING/MONITORING AGENCY NAME(S) AND ADDRESS(ES)
AFOSR/NL
801 N. Randolph Street, Room 732
Arlington, VA 22203-1977

10. SPONSORING/MONITORING AGENCY REPORT NUMBER

11. SUPPLEMENTARY NOTES

12a. DISTRIBUTION AVAILABILITY STATEMENT

Approved for Public Release

12b. DISTRIBUTION CODE

13. ABSTRACT *(Maximum 200 words)*

A novel 1-to-64 (6-bit(2.6)) optical true-time delay module that can provide linear time delays ranging from 0 to 443.03 picoseconds is presented. The total insertion loss, including the propagation loss and the 1-to-64 fan-out loss is confirmed to be less than 20 dB. The crosstalk among channels is measured to be less than - 40 dB. The polarization dependent loss among 64 fan-outs is within 0.37 dB. The bandwidth of the fully packaged module is determined to be as high as 539 GHz. This true-time delay module is employed to control an eight-element K-band phased array antenna system. Far field patterns covering 18 GHz to 26.5 GHz are measured and compared with the simulated results to verify this module's wide instantaneous bandwidth. This module can bee employed to control phased array antennas working at 5 GHz - 40 GHz.

20020614 163

14. SUBJECT TERMS
Phased array antenna, true-time-delay, substrate guided wave, holographic optical element, crosstalk, polarization dependent loss.

15. NUMBER OF PAGES

16. PRICE CODE

17. SECURITY CLASSIFICATION OF REPORT	18. SECURITY CLASSIFICATION OF THIS PAGE	19. SECURITY CLASSIFICATION OF ABSTRACT	20. LIMITATION OF ABSTRACT
UNCLASS	UNCLASS	UNCLASS	

Technical Final report

Contract No. F49620-00-1-0250

Equipment for System Demonstration of Phased Array Antenna using Polymer-based Optical True Time Delay Module

Technical Monitor:

Dr. Charles Lee

AFOSR

Principal Investigator

Ray Chen

University of Texas, Austin

Austin, TX 78758

8/31/2000

Abstract

A novel 1-to-64 (6-bit (2^6)) optical true-time delay module that can provide linear time delays ranging from 0 to 443.03 picoseconds is presented. The total insertion loss, including the propagation loss and the 1-to-64 fan-out loss is confirmed to be less than 20 dB. The crosstalk among channels is measured to be less than –40 dB. The polarization dependent loss among 64 fan-outs is within 0.37 dB. The bandwidth of the fully packaged module is determined to be as high as 539 GHz. This true-time delay module is employed to control an eight-element K-band phased array antenna system. Far field patterns covering 18 GHz to 26.5 GHz are measured and compared with the simulated results to verify this module's wide instantaneous bandwidth. This module can be employed to control phased array antennas working at 5 GHz – 40 GHz.

Index Terms–Phased array antenna, true-time-delay, substrate guided wave, holographic optical element, crosstalk, polarization dependent loss.

I. INTRODUCTION

Phased array antennas (PAAs) have the advantages of low visibility, high directivity and quick steering. Each antenna element of a phased array antenna must have the correct phase condition to accomplish the desired beam scanning. However, the conventional electrical phase trimmer technique is an intrinsic narrow band technique that introduces beam squint. Recently, there has been

growing interest in optical true-time-delay (TTD) modules. Optical TTD techniques are promising for squint-free beam steering of PAAs with features of wide bandwidth, compact size, reduced weights and low electromagnetic interference. Many kinds of optical TTD techniques have been proposed. These include the acoustic-optic technique [1], Fourier optics technique [2], [3], wavelength-multiplexing technique [4], [5], free space techniques [6], [7], planar waveguide techniques [8], [9], [10], fiber delay lines techniques [11], and chirped fiber grating technique [12]. However, these modules are for applications with low RF frequencies, limited resolution and complicated structures for steering control.

In this paper, a new TTD module, having linear time delay steps ranging from 0 to 443.03 picoseconds is designed, fabricated and packaged. The insertion loss and polarization dependent loss (PDL) of this module are measured. The time delay error and bandwidth of the packaged device are specified. This module is employed to control an eight-element K-band PAA system. The wide instantaneous bandwidth of the TTD module is confirmed by measurements of far field patterns covering 18 GHz to 26.5 GHz.

II. STRUCTURE OF THE TTD MODULE

Fig. 1 illustrates the structure of the TTD module. This module is composed of eight sub-units. The optical signal, encoded by a microwave signal, is distributed among the eight sub-units using a 1-to-8 splitter. Each of the sub-units has a

wedge of 21.5 degrees as indicated in Fig. 1. The wedges are coated with total reflect material to ensure that all the optical power is coupled into the substrate. The wedge angle introduces a bounce angle that is larger than the total internal reflection angle (41.8 degrees) at the interface of the substrate (BK-7 glass) and air. Adjacent to each wedge, the height of each sub-unit is maintained at the same value of t. The height of each sub-unit varies after one zig-zag bouncing and maintains at a fixed value for the rest of the sub-unit. Heights of the eight sub-units after the first zig-zag bouncing are from h_1 to h_8, with a difference of ∂h between adjacent sub-units. The difference ∂h is pre-selected to satisfy the required delay combinations. The input signals from single-mode optical fibers are coupled into the module using graded index (GRIN) lenses. The substrate-guided wave zigzags within the substrate through total internal reflection. A portion of the substrate guided wave is extracted out each time the wave encounters the output holographic-grating coupler. The extracted optical waves are focused back into optical fibers using GRIN lenses. From Fig. 1, it can be seen that an eight by eight matrix of time delays is obtained. Fig. 2 shows the two-dimensional view of this TTD module to illustrate how to calculate achievable delay intervals. The position of delay signals in the delay matrix is depicted by (i, j), with i for the row number, j for the column number. Assuming the wedge angle is τ, the introduced time delay between signals at (i, j) and (k, l) is given by

$$\Omega \quad \frac{2n}{c \ \cos(2T)} > l \quad 1 \quad h_k \quad j \quad 1 \quad h_i \cong \qquad (1)$$

where c is the velocity of light in free space, n the refractive index of the substrate, h_i the height of the ith substrate, and h_k the height of the kth substrate.

Dupont photopolymer film HRF600*14-20 is used to form the holographic gratings. BK-7 glass is employed as the guided wave substrates. The surface dimension of each sub-unit is 90mm $\times$ 11mm. The step height t is equal to 2.6 mm. The height difference between the adjacent substrates is 0.147 mm. The heights after the first bouncing of the eight substrates are 3.600 mm, 3.747 mm, 3.894 mm, 4.041 mm, 4.188 mm, 4.335 mm, 4.482 mm, and 4.629 mm, respectively. Therefore, the volume of this module is 90 mm $\times$ 88 mm $\times$ 4.63 mm. The eight by eight two-dimensional time delay matrix is shown in Table 1. The unit of time delays in Table 1 is picosecond. Time delays are calculated in reference to the first column of the delay matrix, providing linear time delays ranging from 0 to 443.03 picoseconds. If the distance interval of a PAA is equal to half of the working wavelength, these time delays can be employed to control PAAs working in the frequency range of 5 GHz – 40 GHz.

The relationship between the time delay interval ∂t and the corresponding antenna steering angle can be expressed as [13]

$$T \quad \sin^{1}(c \ \partial t / d) \qquad (2)$$

where c is the velocity of light in free space, ∂t the time delay interval between adjacent antenna elements, and d the space interval of adjacent antenna elements.

By taking a derivative of the scanning angle with respect to the time delay, we can write the resolution of the scanning angle with respect to the resolution of the time delay interval as

$$IT \quad \frac{c \ It}{d \ \cos T} \qquad (3)$$

where c is the velocity of light in free space, IT the resolution of the scanning angle, It the resolution of the time delay interval, d the space interval of adjacent antenna elements, and T the steering angle of a PAA.

The K-band PAA used in the experiment has eight elements with a spacing interval of 0.3 inch between adjacent elements. By employing the true-time-delay settings for beam-squint-free phased array steering, we are able to calculate possible degrees of the steering of the K-band PAA to be 0, $\pm 4.5^0$, $\pm 9.1^0$, $\pm 13.7^0$, $\pm 18.5^0$, $\pm 23.3^0$, $\pm 28.3^0$, and $\pm 33.6^0$, as long as the columns of the matrix are used to provide delay steps as shown in Table 1. Even wider scanning range can be achieved with more sub-units or higher substrates.

III. CHARACTERISTICS OF THE TTD MODULE

To achieve uniform fan-out beams from each sub-unit, the diffraction equation of the ith and the $i+1$th holograms have to satisfy the following equation.

$$K_{i\ 1} \quad \frac{K_i}{1 \ K_i} \qquad (4)$$

where K_i is the efficiency of the ith holographic-grating coupler, $K_{i\ 1}$ the efficiency of the $i+1$th holographic-grating coupler.

Notice that the achievable maximum efficiency of the HRF600*14-20 photopolymer at 1550 nm is 40%, the efficiencies of the eight holographic-grating couplers on each sub-unit are designed as 10.5%, 11.7%, 13.3%, 15.4%, 18.2%, 22.2%, 28.6%, and 40% sequentially. The corresponding 64 fan-out spots are shown in Fig. 3 in two-dimensional format. In order to further determine the uniformity of the insertion loss, powers of fan-out beams from all eight sub-units are accurately measured, and the total insertion loss, including the propagation loss and the 1-to-64 fan-out loss is experimentally confirmed to be less than 20 dB. The crosstalk between channels is measured to be less then –40 dB.

The polarization sensitivity of fan-out beams of this TTD module is measured employing a polarizer, with the test results shown in Fig. 4. From Fig. 4, it can be seen that the PTL is within 0.37 dB. Therefore, polarization maintained fibers and devices are not required.

The delay intervals are measured using a FPL-01T femtosecond Er-fiber laser from Calmar Optcom Inc., providing optical pulses around 0.2 picoseconds in the vicinity of 1550 nm. Figure 5 illustrates the diagram of the experimental setup for measuring delay intervals. The delay signals are fed into a HP 83480A digital oscilloscope with a resolution of 0.01ps. Since the HP 83480A digital oscilloscope can only detect signals up to 40 GHz, the detected pulses will be broadened to 25 ps. Due to this broadening effect, small delay intervals of several picoseconds can not be shown by the digital oscilloscope. However, since every bouncing inside one sub-unit introduces a same delay, instead of measuring every

delay interval in Table 1, we measured the delay interval between the (1, 8) fan-out and the (8, 8) fan-out. As shown in Fig. 6, the measured delay interval is 98.49 ps, which is the same with the designed value (443.03 ps minus 344.54 ps). Since the module may be used in field demonstration, the temperature effect on the module needs to be evaluated. The index of BK-7 glass has a temperature coefficient (dn/dt) of $5\text{x}10^{-6}$. When the temperature varies from -25^0C to 75^0C ($+/-50^0$C deviation from room temperature), the index will have a change of +/-0.00025. According to Eq. (1), the maximum change of time delay interval happens to the eighth column in Fig. 1, and the change is +/-0.0023 picoseconds. This change generates a maximum scanning shift of +/-1.2 seconds as implied by Eq. (3). This error is so small that it will not degrade the system performance seriously.

In order to determine the maximum frequency range of the microwave signals that can be carried by the TTD module, the bandwidth of the packaged device is specified. There are three main factors that decide the dispersion capacity of this TTD module. One is the dispersion caused by holographic grating couplers. The second factor comes from the dispersion of GRIN lens and optical fibers. The third one is material dispersion caused by different phase velocities of different wavelengths. To evaluate the real bandwidth of this TTD module, a femtosecond laser and the Fourier spectrum analysis method are employed [21]. The same femtosecond laser is used as in the delay measurement. A FR-103MN autocorrelator from Femtochrome research Inc. is adopted to measure pulse

widths before and after passing the fully packaged TTD module. The output signal from the autocorrelator is processed and displayed by a computer. Fig. 7(a) depicts the autocorrelation traces of the reference and dispersed pulses respectively. Fourier transform of the two pulses generates bandwidth information of this TTD module, as shown in Fig. 7(b). As can be seen in Fig. 7(b), the 3dB bandwidth of the device is 539GHz.

IV. SYSTEM STRUCTURE

The packaged TTD module is shown in Fig. 8 with one column fan-out coupled out. The integrated K-band PAA system is demonstrated in Fig. 9. Fig. 9(a) shows the transmission part of the system. Fig. 9(b) shows both the transmitter and horn antenna receiver. A microwave signal is generated by the heterodyne technique using two external cavity tunable semiconductor lasers. The optical carriers are evenly distributed among the eight sub-units of the TTD module by a 1-to-8 splitter. Desired time delays are added by this TTD module. In order to have a reference plane, a pre-adjustment delay bank is inserted at this point to compensate for the different delays caused by devices other than this TTD module. Afterwards, the microwave signals are detected by InGaAs high-speed photodetectors. The eight microwave signals with correct phase relationship are fed into eight antenna elements individually after amplification. The on/off states of photodetectors are controlled by a printed circuit board, which also serves as a microwave power uniformity controller. For single angle scanning of this K-band

PAA, only one column of the fan-out beams from the TTD module is utilized. When the module is used as a beamforming network, all 64 fan-out beams from the TTD module are fed into 64 photodetectors, and all photodetectors are in the "on" states. Furthermore, microwave signals detected from the same row of the TTD module are first combined before they are fed to the PAA.

V. FAR FIELD PATTERN MEASUREMENTS

Far field patterns of the K-band PAA are measured to verify the instantaneous microwave broad bandwidth. Various delay combinations are tested. Far field patterns are measured at three frequencies, the center frequency (22 GHz) and two edge frequencies (18 GHz, and 26.5 GHz). Fig. 10 compares the far field patterns at the three frequencies, with solid curves and curves with triangles denoting simulated results and measured results respectively. Note that in Fig.10, the fifth column of the TTD module shown in Fig.1 is employed to provide delay control signals for 18.5^{0} scanning of the PAA. The locations of the main lobes covering all K band resulted from simulation and experiment agree very well. Furthermore, the PAA scanning angle is independent of microwave frequencies over the entire K-band, a primary feature of the true-time-delay approach.

VI. CONCLUSION

In conclusion, a novel 6-bit optical TTD module that can provide 0 to 443.03 picoseconds time delay has been fabricated, packaged and integrated into a

K-band PAA system. This module has insertion loss of less than 20 dB, a crosstalk of less than –40 dB, a PDL of 0.37 dB, and a bandwidth of 539 GHz. This module is compact, easy to fabricate, and experimentally confirmed to provide a wide instantaneous microwave bandwidth. Furthermore, this module can be employed to control phased array antennas working at 5 GHz – 40 GHz.

This research is currently supported by the AFOSR, BMDO, 3M Foundation, and the Advanced Technology Program of the State of Texas.

REFERENCES

[1] L.H. Gesell, R.E. Feinleib, J.L. Lafuse, and T. M. Turpin, "Acousto-optic control of time delays for array beam steering," *Optodelctronic Signal Processing for Phased-Array Antennas IV, Proc. SPIE,* vol. 2155, pp. 194-204, 1994.

[2] Yoshihiko Konishi, etc., "Carrier-to-Noise Ratio and Sidelobe Level in a Two-Laser Mode Optically Controlled Array Antenna Using Fourier Optics", *IEEE Trans. on Antennas and Propagation*, vol. 40, pp. 1459-1465, 1992.

[3] G. A. Koepf, Optical processor for phased-array antenna beam formation, *Proc. SPIE*, vol. 477, pp. 75-81, 1984.

[4] D.T.K. Tong and M.C. Wu, "A novel multiwavelength optically controlled phased array antenna with a programmable dispersion matrix," *IEEE Photonics Technol. Lett.* Vol. 8, pp. 812-814, 1996.

[5] R. Esman, M.Frankel, J. Dexter, L. Goldberg, M. Parent, D. Stiwell, and D. Cooper, "Fiber-optic prism true time-delay antenna feed," *IEEE Photonics*

Technol. Lett., vol. 5, pp. 1347-1349, 1993.

[6] H. R. Fetterman, Y. Chang, D. C. Scott, S. R. Forrest, F. M. Espiau, M. Wu, D. V. Plant, J. R. Kelly, A. Matteer, and W. H. Steier, "Optically controlled phased array radar receiver using SLM switched real time delays," *IEEE Microwave Guid. Wave Lett.*, vol. 5, pp. 414-416, 1995.

[7] D. Dolfi, P. Joffre, J. Antoine, J. Huignard, D. Phillippet, and P. Granger, "Experimental demonstration of a phased-array antenna optically controlled with phase and time delays," *Appl. Opt.*, vol. 35, pp. 5293-5300, 1996.

[8] E. Ackerman, S. Wanuga, D. Kasemset, W. Minford, N. Thorsten, and J. Watson, "Integrated 6-bit photonic true-time-delay unit for lightweight 3-6GHz radar beamformer," *IEEE Trans. Microwave Theory Tech.,* vol. 6, pp. 681-684, 1992.

[9] Kohji HORIKAWA, Ikuo OGAWA, Hiroyo OGAWA, and Tsutomu KITOH, Photonic Switched True Time Delay Beam Forming Network Integrated on Silica Waveguide Circuits, *IEEE MTT-S Dig.*, TU1C-6, pp. 65-68, 1995.

[10] Wenshen Wang, Yongqiang Shi, Weiping Lin, and James H. Bechtel, Waveguide Binary Photonic True-Time Delay Lines Using Polymer Integrated Switches and Waveguide Delays, *Proc. SPIE*, vol. 2844, pp. 200-211, 1996.

[11] W. Ng, A. A. Walston, G. L. Taughlian, J. J. Lee, I. L. Newberg and N. Bernstein, "The first demonstration of an optically steered microwave phased array antenna using true-time-delay," *J. Lightwave Technol*, vol. 9, pp. 1124-1131, 1991.

[12] Juan L. Corral, Javier Marti, "Optical Up-Conversion on Continuously Variable True-Time-Delay Lines Based on Chirped Gratings for Millimeter-Wave Optical Beamforming Networks", *IEEE Trans. On Microwave theory and techniques*, vol. 47, pp, 1315-1320, 1999.

[13] A.A. Oliner and G. H. Knittel, *Phased Array Antennas.* Norwood, Mass.: Artech House, 1972.

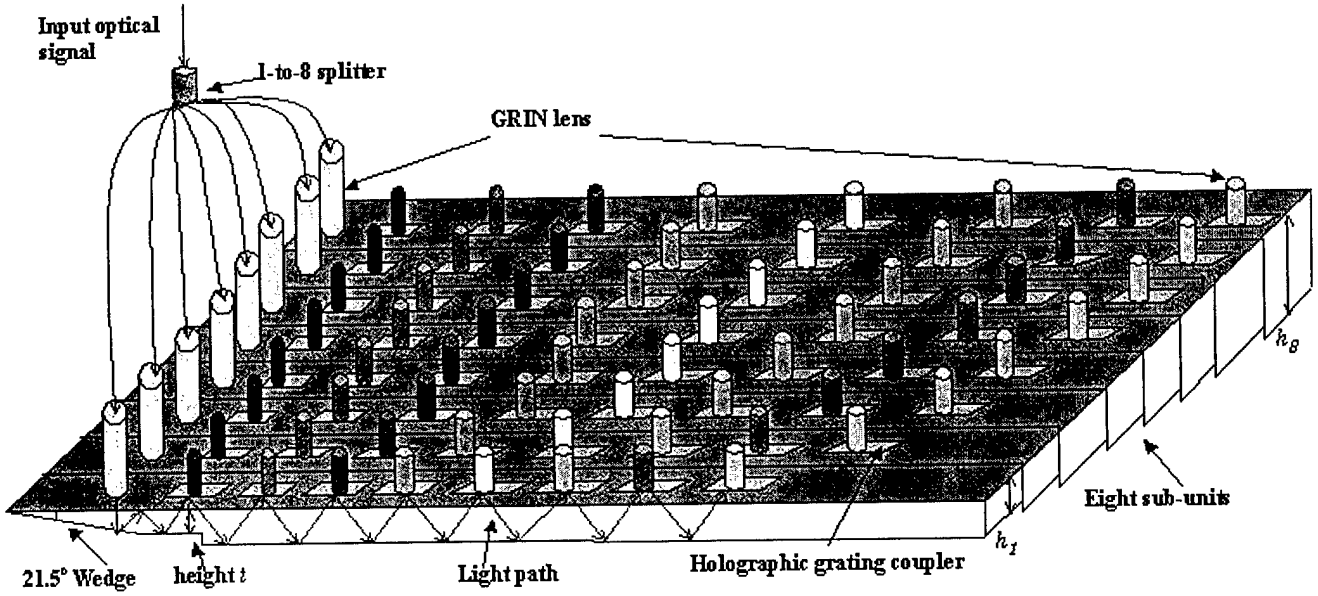

Fig. 1. Diagram of the structure of the 6-bit TTD module based on substrate-guided wave and holographic-grating couplers. GRIN, graded index.

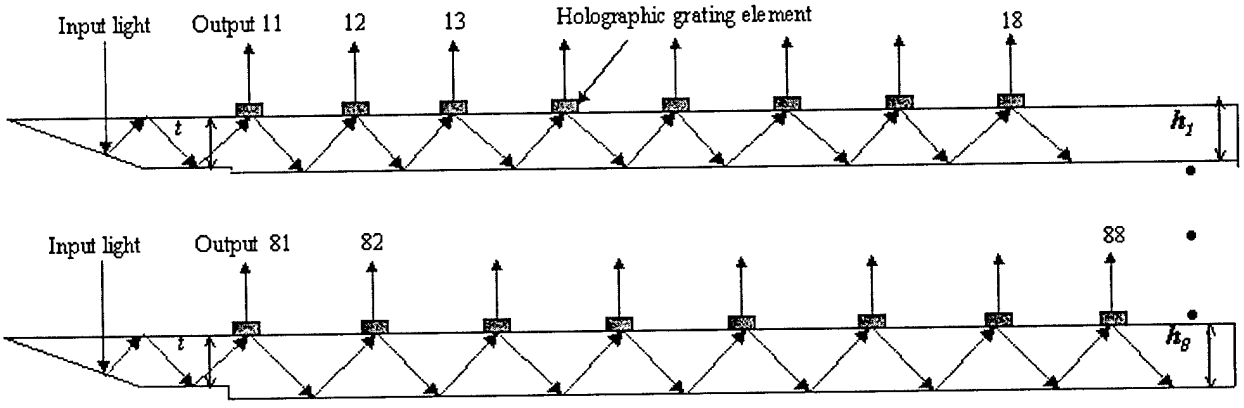

Fig. 2. The two-dimension view of the TTD module.

Column / Row	1	2	3	4	5	6	7	8
1	0	49.22	98.44	147.66	196.88	246.10	295.32	344.54
2	0	51.23	102.46	153.69	204.92	256.15	307.38	358.61
3	0	53.24	106.48	159.72	212.96	266.20	319.44	372.68
4	0	55.25	110.50	165.75	221.00	276.25	331.50	386.75
5	0	57.26	114.52	171.78	229.04	286.30	343.56	400.82
6	0	59.27	118.54	177.81	237.08	296.35	355.62	414.89
7	0	61.28	122.56	183.84	245.12	306.40	367.68	428.96
8	0	63.29	126.58	189.87	253.16	316.45	379.74	443.03
Delay steps	0	2.01	4.02	6.03	8.04	10.05	12.06	14.07
Scan angles	0^0	$\pm 4.5^0$	$\pm 9.1^0$	$\pm 13.7^0$	$\pm 18.5^0$	$\pm 23.3^0$	$\pm 28.3^0$	$\pm 33.6^0$

Unit of time delay: Picosecond

Table 1. The delay matrix and corresponding scanning angles of the TTD module.

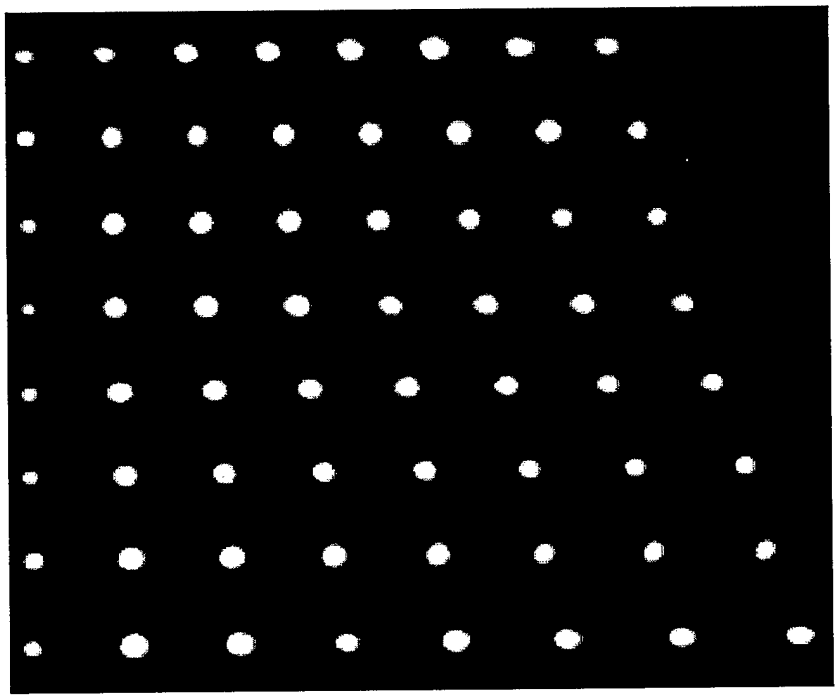

Fig. 3. Sixty-four fan-outs from the TTD module.

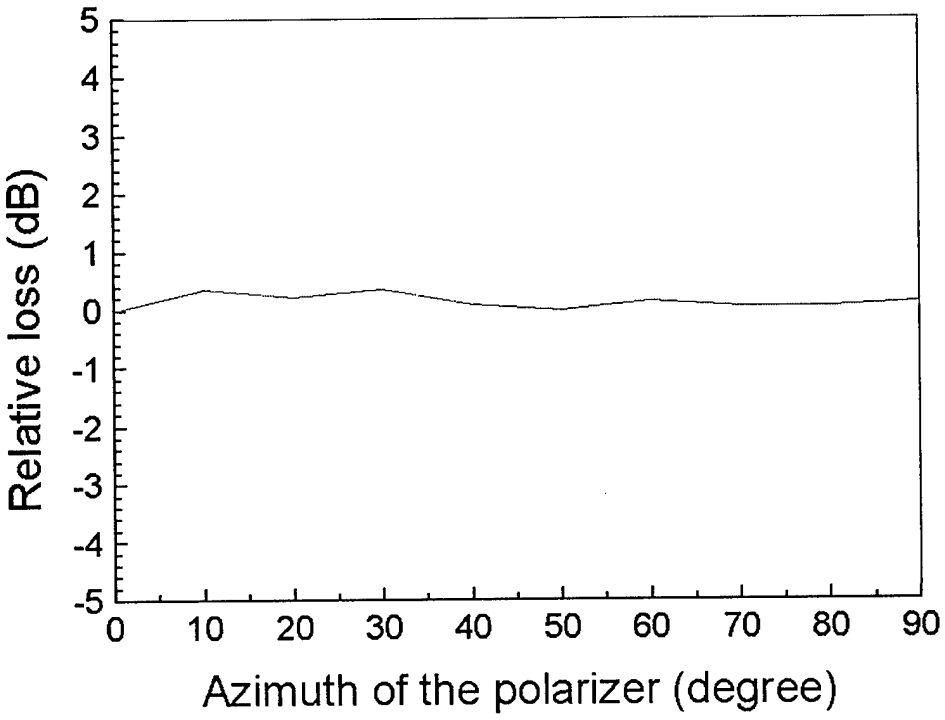

Fig. 4. Polarization dependent loss (PDL) of the TTD module.

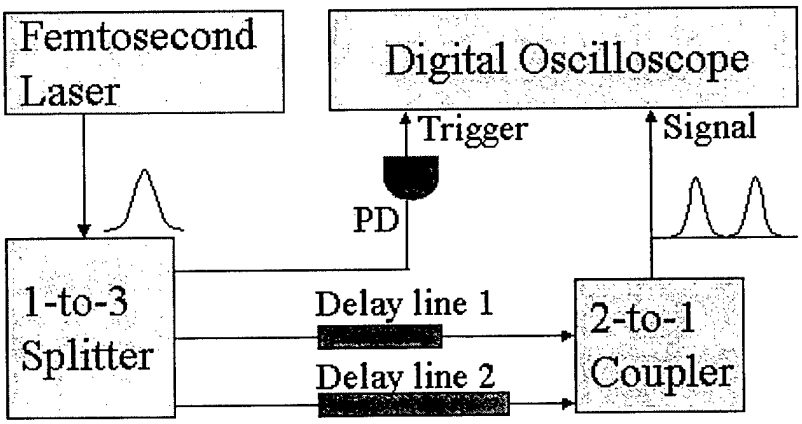

Fig. 5. Diagram of the experimental setup for measuring delay intervals.

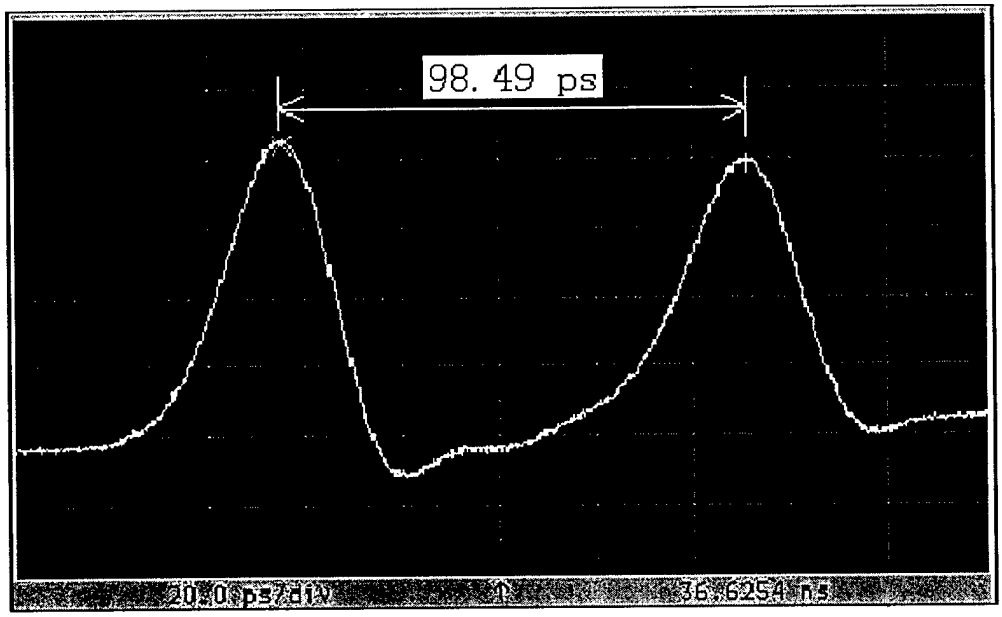

Fig. 6. Measured delay interval between (1, 8) fan-out and (8, 8) fan-out.

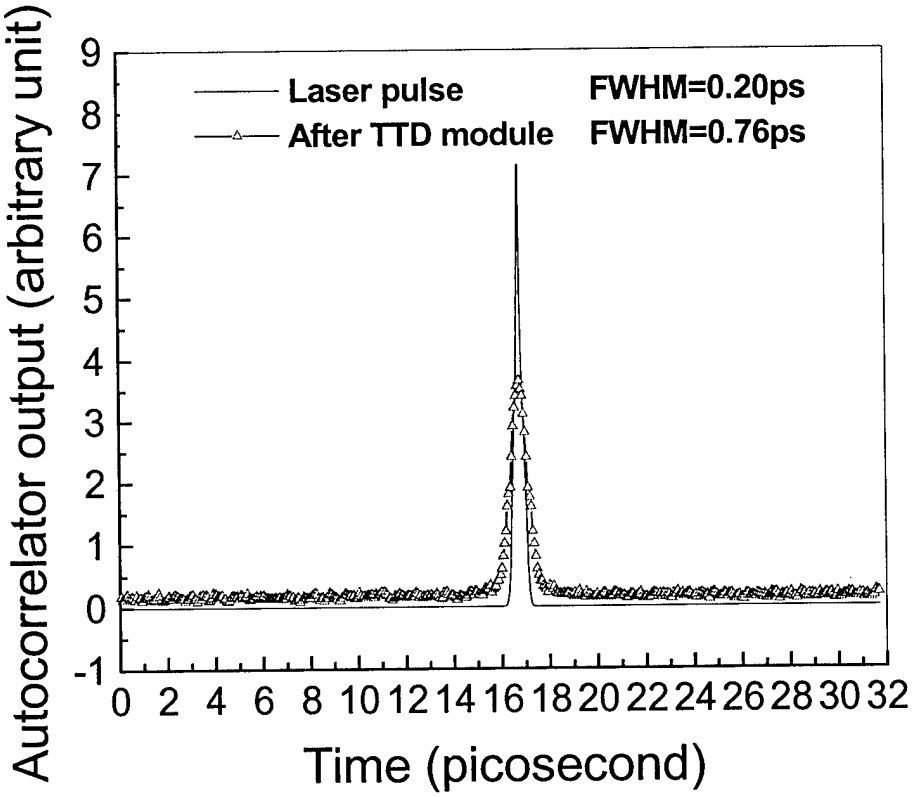

Fig. 7. (a) Autocorrelation traces of the pulses before and after passing the TTD module.

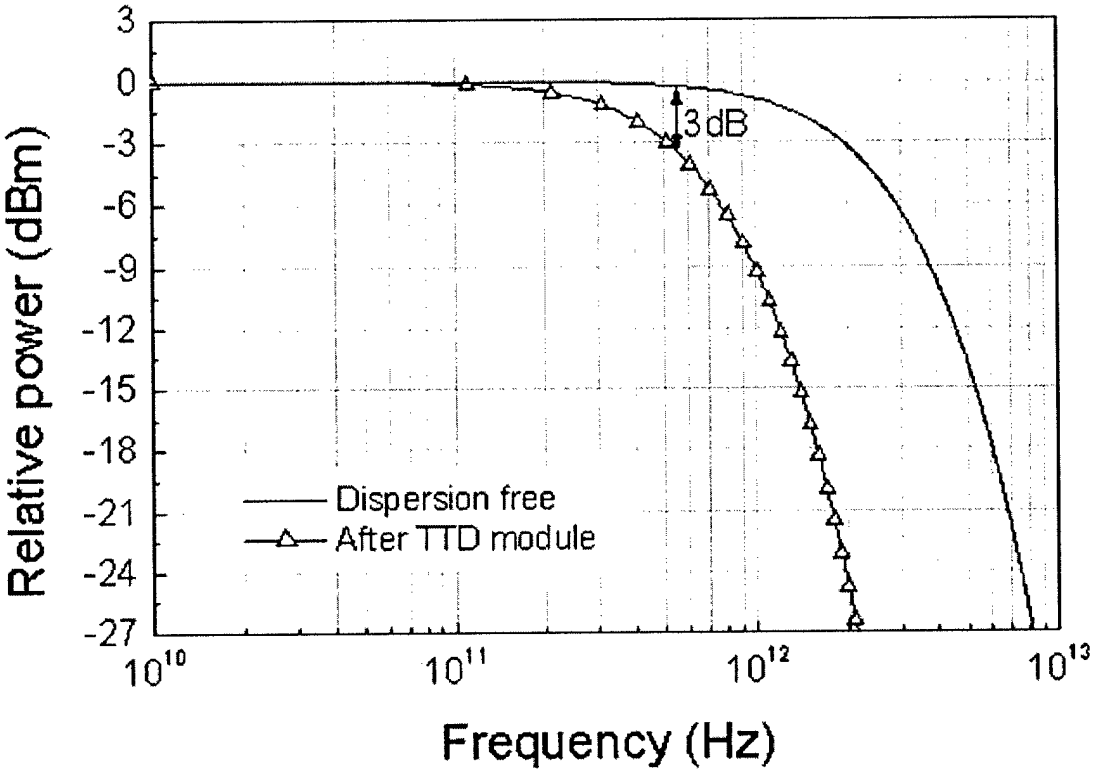

Fig. 7. (b) FFT power spectrum for the reference and dispersed pulses.

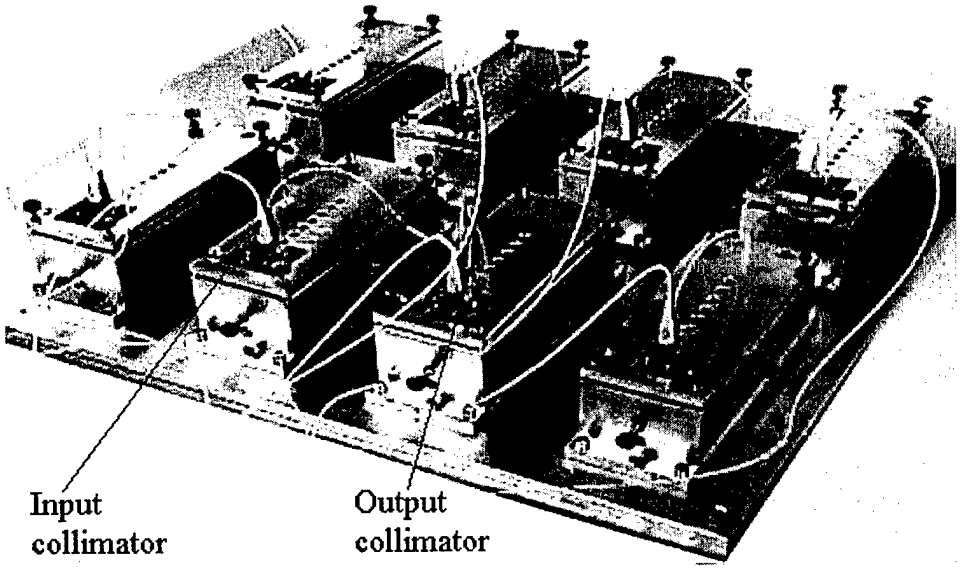

Fig. 8. Photograph of the packaged 8-bit TTD module.

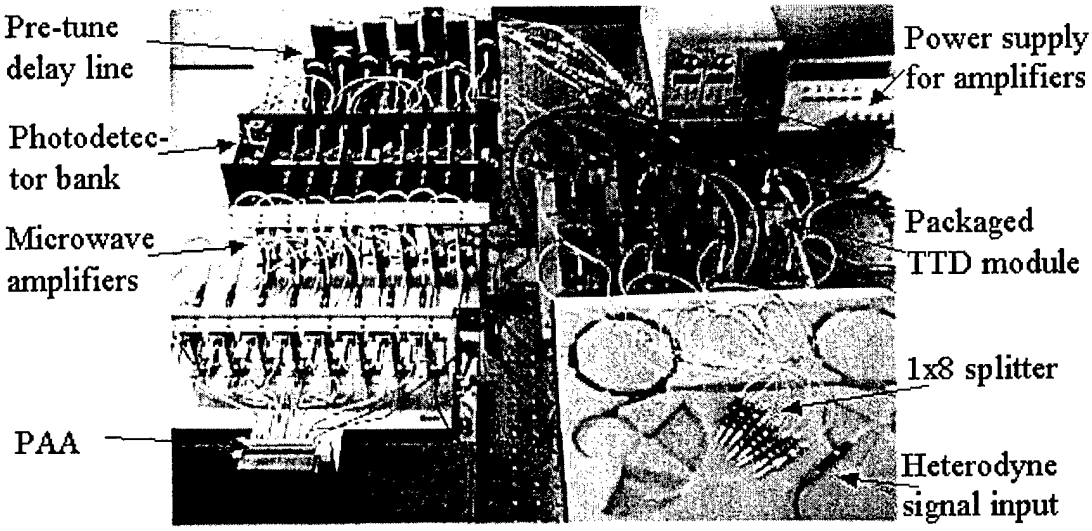

Fig. 9. Photograph of integrated K-band PAA system

(a) Photograph of the transmission part of the PAA system

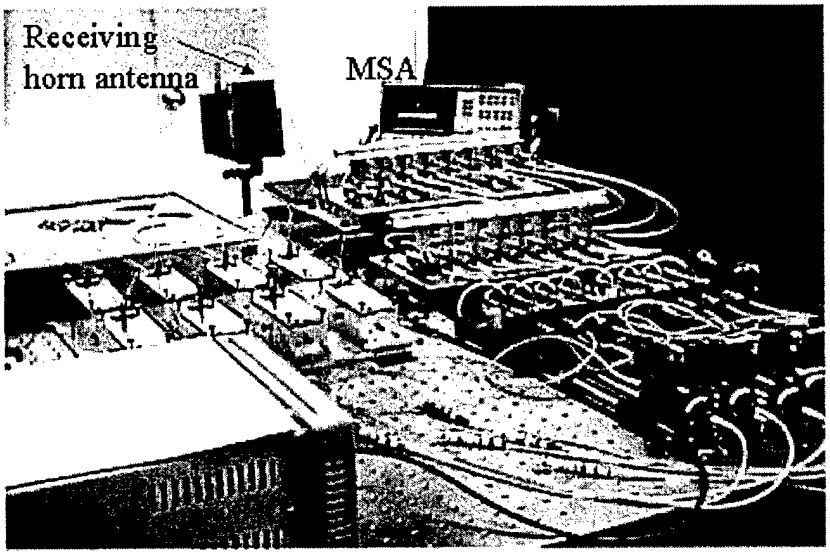

Fig. 9. Photograph of integrated K-band PAA system

(b) Photograph of the PAA system with a standard horn receiver.

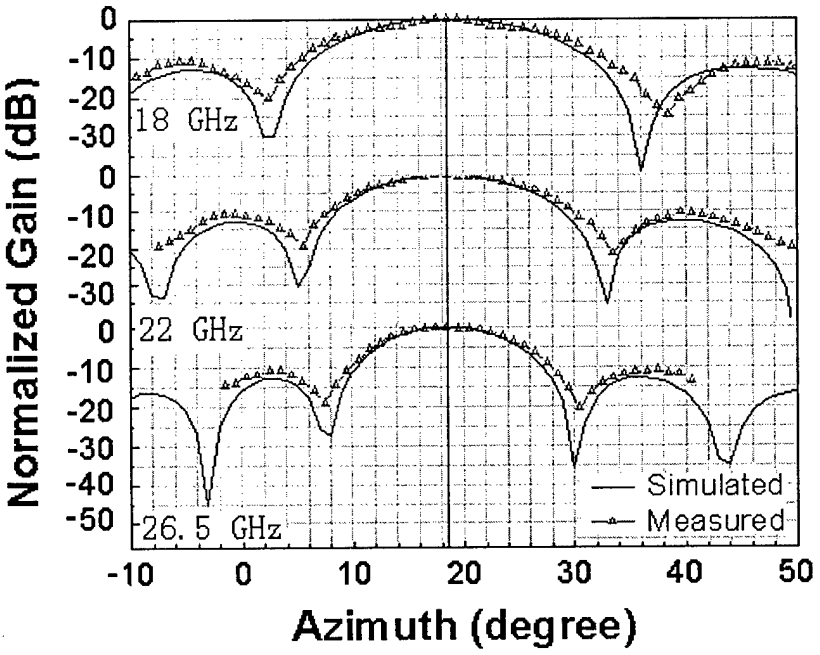

Fig. 10. Comparison of far field patterns at three different frequencies: 18 GHz, 22 GHz, and 26.5 GHz.